JPEDAV (2005) 26:124-130
DOI: 10.1361/15477030522860
1547-7037/$19.00 ©ASM International

Thermodynamic Properties of 1-Butyl-3-Methylimidazolium Chloride (C_4mim[Cl]) Ionic Liquid

Mingming Zhang, Venkat Kamavaram, and Ramana G. Reddy

(Submitted August 6, 2004; in revised form December 27, 2004)

Thermodynamic properties of 1-butyl-3-methylimidazolium chloride (C_4mim[Cl]) ionic liquid were determined using thermogravimetric (TG) differential thermal analysis (DTA). A new method called DTA mass-difference baseline, was used to measure the heat capacity and enthalpy change of phase transformation of ionic liquid from DTA curves. Based on this, the changes in standard enthalpy, entropy, and Gibbs energy were determined. The results show that standard enthalpy and entropy changes of C_4mim[Cl] increase nonlinearly with increasing temperature, while the standard Gibbs energy change decreases nonlinearly with increasing temperature within the temperature range studied (298-453 K). The standard enthalpy of melting and enthalpy of vaporization were determined to be 0.93 and 11.07 kJ/mol, respectively.

1. Introduction

Ionic liquids are a class of organic salts that are liquids in their pure state at or near room temperature. They exhibit many interesting properties such as negligible vapor pressure, low melting point, and wide liquid range. Due to their unique combination of properties, ionic liquids have been studied for several electrochemical applications.[1] Evaluation of physical and chemical properties of these ionic liquids is essential for their commercial applications.[2] Only in the recent years has significant literature on heat capacities of ionic liquids become available.[3] However, to the best of our knowledge, no literature is available on the measurement of thermodynamic properties such as enthalpy, entropy change with temperature, and enthalpy of phase transformation of chloride ionic liquids.

The enthalpy change of ionic liquids with temperature generally consists of three parts; enthalpy of melting or glass transition, heat capacity, and enthalpy of vaporization or pyrolysis. Studying the variation of overall enthalpy and its three individual components with temperature will provide important information for the application of ionic liquids in several electrochemical and energy conversion fields.

Holbrey et al. have determined heat capacities of several common ionic liquids containing 1-alkyl-3-methylimidazolium cations from 303 to 453 K using modulated differential scanning calorimetry (DSC).[3] It was reported that heat capacity followed a linear relationship $C_p = k + aT$. However, enthalpy of melting or glass transition and enthalpy of vaporization (or pyrolysis) of these ionic liquids were not measured, mainly due to the limitation of DSC system, which requires a constant sample mass throughout the measurement.

One of the significant advantages of ionic liquids is their high thermal stability, which enables their application over a wide operating temperature range. Reddy et al. have reported the long term thermal stability of several common ionic liquids.[4] They observed that 1-butyl-3-methylimidazolium chloride (C_4mim[Cl]) starts to degrade at 523 K, whereas decomposition of 1-butyl-3-methylimidazolium bis(trifluoromethanesulfonyl)imide (C_4mim[Tf_2N]) begins at 723 K. Thermal stabilities of di-alkylimidazolium-based salts were strongly dependent on salt structure and the relative anion stabilities were observed as $Tf_2N^- > PF_6^- > BF_4^- \gg Cl^-$.[5]

In the current study, heat capacity and standard enthalpy change of C_4mim[Cl] ionic liquid were determined using the differential thermal analysis (DTA) mass-difference baseline method.[6,7] The theoretical correlation between DTA signal, enthalpy change, and heat transfer process was obtained by calibrating the DTA equipment using pure α-sapphire as a standard material. The standard entropy and Gibbs energy change of the ionic liquid was subsequently calculated from enthalpy data in the temperature range of 298-453 K. The data generated in this study could be added to the database of thermodynamic properties of ionic liquids.

2. Experimental

2.1 Preparation of Ionic Liquids

The ionic liquid C_4mim[Cl] was synthesized according to standard procedures described elsewhere.[2,8,9] Starting materials, 1-methylimidazole (redistilled, 99+% pure), and 1-chlorobutane (99.5% pure, anhydrous), were obtained from Sigma Aldrich (Milwaukee, WI). After synthesis, the

Mingming Zhang and **Venkat Kamavaram,** Department of Metallurgical and Materials Engineering, The University of Alabama, Tuscaloosa, AL 35487; and **Ramana G. Reddy,** ACIPCO Professor and Associate Director of Center for Green Manufacturing, Department of Metallurgical and Materials Engineering, The University of Alabama, Tuscaloosa, AL 35487. Contact e-mail: rreddy@coe.eng.ua.edu.

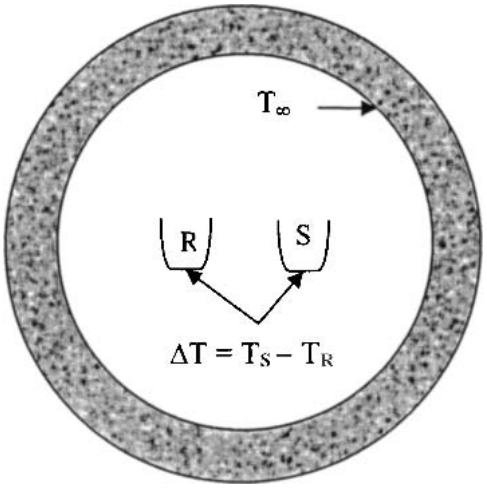

Fig. 1 Schematic setup of TG/DTA furnace with horizontal balance beams

liquid was dried under vacuum at 70 °C for 24 h to remove any unreacted chemicals and wash solvent.

2.2 Thermogravimetric DTA Measurements

A Perkin Elmer Pyris Diamond TG/DTA (Boston, MA) was used in the current study for the DTA measurements. Figure 1 illustrates the typical horizontal balance beam setup of a thermogravimetric (TG)/DTA apparatus. A constant heating rate of 10 °C/min and high-purity argon purge (100 cm^3/min) were used for all the measurements. Each ionic liquid sample was dried under vacuum for two hours before conducting the TG/DTA measurements. The reference material was sapphire (α-Al_2O_3), and both reference and sample pans were made of platinum. The standard material used for calibrating the equipment was α-sapphire powder (Perkin Elmer).

2.3 Theory of DTA Mass-Difference Baseline Method

DTA measures the temperature difference between the sample (T_s) and the reference (T_r) materials, $\Delta T = T_s - T_r$, which is then converted to enthalpy change (ΔH) using a conversion factor. DTA signal represents the change in temperature difference between the sample and the reference material. The relationship between a DTA signal and enthalpy change can be determined from the theory developed by Vold.[10]

The energy balance on the sample side is given by the following equation:

$$m_p C_{P,p} \frac{dT_s}{dt} + m_s C_{P,s} \frac{dT_s}{dt} + m_s \frac{dQ}{dt} = \alpha_s A_s (T_\infty - T_s) \qquad \text{(Eq 1)}$$

where t is time; m_p and $C_{P,p}$ are mass and heat capacity of pan for both the reference and sample sides; m_s and $C_{P,s}$ are mass and heat capacity of the sample; Q is the transition heat produced by phase change or chemical reaction; α_s is the overall heat transfer coefficients from furnace to sample side; A_s is the surface area of the sample; and T_∞ is the furnace temperature. Now, with an empty reference pan, the energy balance on reference side is given by Eq 2:

$$m_p C_{P,p} \frac{dT_r}{dt} = \alpha_r A_r (T_\infty - T_r) \qquad \text{(Eq 2)}$$

where α_r is the overall heat transfer coefficients from furnace to reference side, and A_r is the surface area of reference. Subtracting Eq 2 from Eq 1 and substituting the following relations $\Delta T = T_s - T_r$ and $dH/dt = C_{P,s}(dT_s/dt) + dQ/dt$, we arrive at:

$$\frac{m_s dH}{dt} + \frac{m_P C_{P,p} d(\Delta T)}{dt} = \alpha_s A_s (T_\infty - T_s) - \alpha_r A_r (T_\infty - T_r) \qquad \text{(Eq 3)}$$

By assuming $A = A_s = A_r$, the right hand side of the above equation can be simplified to Eq 4:

$$\alpha_s A(T_\infty - T_s) - \alpha_r A(T_\infty - T_r) = (\alpha_s - \alpha_r)A(T_\infty - T_r) - \alpha_s A(T_s - T_r) \qquad \text{(Eq 4)}$$

Substitution of Eq 4 into Eq 3 with further simplification yields Eq 5:

$$\Delta T = \frac{(\alpha_s - \alpha_r)}{\alpha_s}(T_\infty - T_r) - \frac{m_s dH}{\alpha_s A dt} - \frac{m_P C_{P,p} d(\Delta T)}{\alpha_s A dt} \qquad \text{(Eq 5)}$$

The last term on the right hand side of the above equation can be omitted since it is much smaller than the other two terms, and Eq 5 can be transformed to Eq 6:

$$\Delta T = \frac{(\alpha_s - \alpha_r)}{\alpha_s}(T_\infty - T_r) - \frac{m_s dH}{\alpha_s A dt} \qquad \text{(Eq 6)}$$

From Eq 6, temperature difference (ΔT) can be determined by enthalpy change ΔH, and heat transfer difference between sample and reference $(\alpha_s - \alpha_r)(T_\infty - T_r)$. It was reported that heat transfer influence can be eliminated by a simple assumption that $(\alpha_s - \alpha_r)$ equals zero,[11] which is impractical for a measurement over a wide range of temperatures.

To quantitatively determine enthalpy change over a wide temperature range, the DTA mass-difference baseline method was selected.[6,7] This method uses the DTA curve of the sample, the mass of which is in the lower limit for the equipment, as baseline for DTA measurements. Asymmetric heat transfer influence on both sample and reference sides can be minimized by subtracting a baseline constructed by a smaller weight sample under similar conditions. This method improves the linearity between DTA signal and enthalpy change. Figure 2 illustrates the heat capacity measurements of α-sapphire obtained using the above method. Curve (a) (m = 5.0 mg) was used as baseline for curve (b) (m = 21.0 mg). A similar trend for both curves during temperature evolution indicates a similar heat transfer coefficient α_s. The DTA signal for curve (a) was more intense than that for curve (b). Hence, with similar

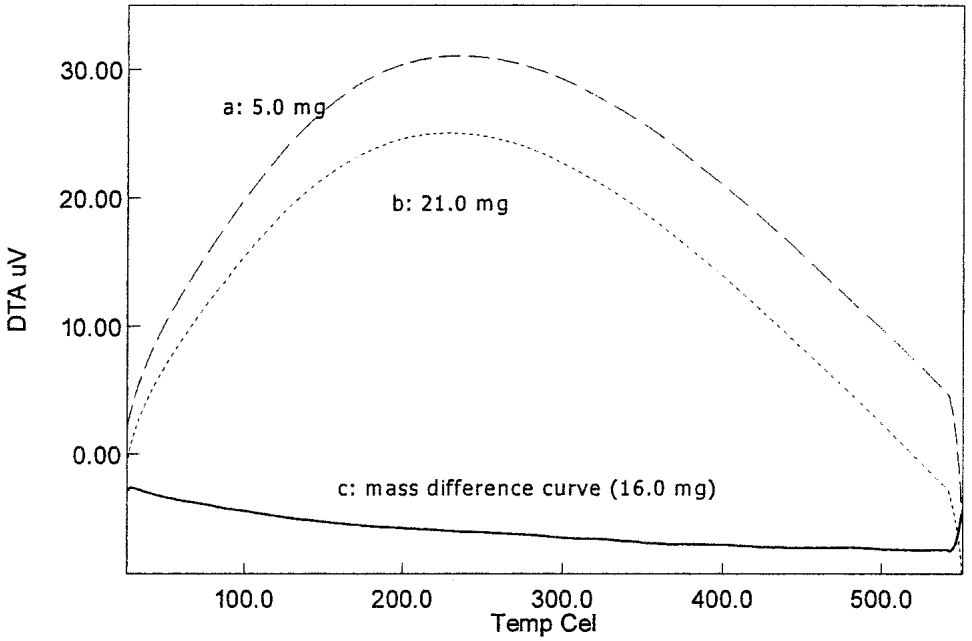

Fig. 2 Heat capacity measurement of α-sapphire using the mass difference baseline method. Curve (a): DTA curve of α-sapphire with $m = 5.0$ mg. Curve (b): DTA curve of α-sapphire with $m = 21.0$ mg. Curve (c): area between curves (a) and (b)

heat transfer coefficient (α_s) for both baseline and sample DTA signals, the temperature difference between them can be expressed as follows:

$$\Delta T_1 - \Delta T_2 = \left(\frac{(\alpha_{s,1} - \alpha_{r,1})}{\alpha_{s,1}} - \frac{(\alpha_{s,2} - \alpha_{r,2})}{\alpha_{s,2}}\right)(T_\infty - T_r) - \frac{m_{s,1}\mathrm{d}H}{\alpha_{s,1}A\mathrm{d}t} + \frac{m_{s,2}\mathrm{d}H}{\alpha_{s,2}A\mathrm{d}t} \quad \text{(Eq 7)}$$

$$\Delta T_1 - \Delta T_2 = \frac{(m_{s,2} - m_{s,1})\mathrm{d}H}{\alpha_s A\mathrm{d}t} \quad \text{(Eq 8)}$$

where ΔT_1 and ΔT_2 are temperature differences between the sample and the reference material for different samples of masses $m_{s,1}$ and $m_{s,2}$ ($m_{s,1} < m_{s,2}$), respectively. For a DTA measurement, the heating rate is usually fixed, $\mathrm{d}T = \mathrm{K}\mathrm{d}t$, $\Delta T = \mathrm{K}_2 D$, where D refers to a DTA signal and it is assumed that $\mathrm{K}_1 = \alpha_s A$. On simplification (Eq 8) yields:

$$\frac{\mathrm{d}H}{\mathrm{d}T} = \frac{\mathrm{K}_1\mathrm{K}_2}{\mathrm{K}}\frac{(D_1 - D_2)}{(m_{s,2} - m_{s,1})} \quad \text{(Eq 9)}$$

where $(D_1 - D_2)$ is the difference between two DTA signals; $(m_{s,2} - m_{s,1})$ is the mass difference between two samples; K is the heating rate constant; K_1 is the heat transfer constant, which depends on the sample properties and the operating conditions; and K_2 is the apparatus related parameter, which is only a function of temperature. In this work, the enthalpy change of α-sapphire powder was measured over the temperature range 300-720 K and was compared with the literature data for determining the conversion factor for relating the DTA signal and enthalpy change over the temperature range studied.

2.4 Calibration of DTA Equipment for Enthalpy Measurement

Since the heating rate is constant throughout the measurement, K is constant, and when the sample properties and operating conditions are fixed for each test, K_1 can be assumed to be constant. Based on the above assumptions, Eq 9 can be simplified to yield the following correlation[6,11]:

$$\left(\frac{\mathrm{K}_2}{\mathrm{K}_2'}\right) = \frac{D'}{D}\frac{(\mathrm{d}H/\mathrm{d}T)}{(\mathrm{d}H/\mathrm{d}T')} \quad \text{(Eq 10)}$$

where $(\mathrm{K}_2/\mathrm{K}_2')$ is a function of temperature, which can be determined for a standard material, and is subsequently used for DTA tests of other materials. The enthalpy change can be calculated from the DTA signal by simplifying the above equation as:

$$\frac{\mathrm{d}H}{\mathrm{d}T} = \frac{\mathrm{K}_2}{\mathrm{K}_2'}\frac{(\mathrm{d}H/\mathrm{d}T)'}{D'}D \quad \text{(Eq 11)}$$

Expressions ($\mathrm{d}H/\mathrm{d}T$, D) with primes ($'$) refer to standard material, and those without primes refer to the sample material. If all the quantities are substituted into Eq 11, $\mathrm{d}H/\mathrm{d}T$ of the sample material can be determined.

2.5 Determination of Conversion Factor (K_2/K_2')

Pure α-sapphire was used as a standard material to calculate the conversion factor ($\mathrm{K}_2/\mathrm{K}_2'$). Table 1 shows the

Table 1 Conversion factor [$K_2/K_2' = f(T)$] determined using α-sapphire as standard

T, K	C_p, J/mol · K(a)	C_p/C_p'(b)	DTA, μV	DTA/DTA′(c)	K_2/K_2'
300	79.41	1.00	−2.82	1.00	1.00
320	83.46	1.05	−3.24	1.15	0.91
330	85.09	1.07	−3.57	1.27	0.83
340	87.16	1.10	−3.73	1.32	0.83
360	90.45	1.14	−4.20	1.49	0.76
370	91.97	1.16	−4.36	1.55	0.75
380	93.41	1.18	−4.56	1.62	0.73
400	96.08	1.21	−4.94	1.75	0.69
420	98.49	1.24	−5.23	1.85	0.67
440	100.69	1.27	−5.48	1.94	0.65
460	102.67	1.29	−5.68	2.01	0.64
480	104.48	1.32	−5.81	2.06	0.64
500	106.12	1.34	−5.96	2.11	0.63
520	107.63	1.36	−6.08	2.16	0.63
540	109.02	1.37	−6.21	2.20	0.62
560	110.28	1.39	−6.37	2.26	0.61
580	111.45	1.40	−6.58	2.33	0.60
600	112.54	1.42	−6.66	2.36	0.60
620	113.54	1.43	−6.86	2.43	0.59
640	114.47	1.44	−7.05	2.50	0.58
660	115.35	1.45	−7.03	2.49	0.58
680	116.15	1.46	−7.12	2.52	0.58
700	116.92	1.47	−7.25	2.57	0.57
720	117.63	1.48	−7.33	2.60	0.57

(a) Standard material, α-sapphire. (b) C_p' is the heat capacity of α-sapphire at $T = 300$ K. (c) DTA′ is the measured DTA value at $T = 300$ K.

measured DTA data, the heat capacity data from the literature,[12] and the conversion factor calculated from Eq 10. Considering the thermal stability of α-sapphire, 300 K was chosen as the starting point for conversion factor determination. DTA measurements were made for two samples of different mass using the same reference material (Al_2O_3) from 300 K to 720 K. Figure 2 shows the DTA curves for samples (a) ($m_a = 5.0$ mg) and (b) ($m_b = 21.0$ mg), and it can be seen that both curves increase in a similar manner with increasing temperature. However, the two DTA signals have different magnitudes due to the mass difference (Fig. 2). Curves (a) and (b) refer to positive DTA signals in the temperature range of study, indicating a heat transfer on the sample side larger than that on the reference side. Moreover, they vary nonlinearly with temperature, implying a complex relationship between the heat transfer coefficient and the environmental conditions. The enthalpy change of a sample of mass ($m_b - m_a = 16.0$ mg) is represented by curve (c) in Fig. 2. Apparently, the subtracted DTA curve shows a nearly linear variation with temperature as a result of elimination of heat transfer influences between the sample and reference sides.

2.6 Enthalpy Measurement

Figure 3 shows the TG/DTA curves for C_4mim[Cl] with an argon (ultra-high purity [UHP], 100 cm^3/min) flow. In Fig. 3, two distinct endothermic peaks can be seen at 330 and 588 K, which correspond to melting and vaporization phase changes (or pyrolysis), respectively. With standard analysis software (Muse V.2.5U, Seiko Instruments Inc., Mihama-Ku, Chiba-Shim Chiba, Japan) common tangents are constructed at each distinct peak for the enthalpy calculation. Qualitatively, the enthalpy change during the transformation can be related to the area under the tangent of the DTA peak. However, a conversion factor is necessary to convert the DTA peak area to enthalpy of transformation. As mentioned in the previous section, the conversion factor was determined using α-sapphire as a standard material.

Figure 4 illustrates the DTA curves of C_4mim[Cl] for two different masses (20.56 and 14.38 mg). The mass difference DTA curve is also plotted in Fig. 4. The common tangent drawn to the mass difference curve can also be seen in Fig. 4. From Fig. 4, a small difference in melting peaks and a large difference in vaporization peaks can be observed in the DTA curves obtained for different masses. As mentioned in the above paragraph, the three distinct regions observed in each DTA curve can be related to their corresponding enthalpy changes, e.g., enthalpy of melting, heat capacity change, and enthalpy of vaporization (or pyrolysis).

3. Thermodynamic Calculations

Evaluation of thermodynamic properties of ionic liquids is essential for their application in thermal storage and heat transfer industry. Based on the heat capacity and standard enthalpy change data, the changes in standard entropy and Gibbs energy of ionic liquid over a temperature range of 298-453 K can be calculated. The changes in standard enthalpy and entropy of C_4mim[Cl] take into consideration the phase changes, i.e., melting (or glass transition) and evaporation, Eq 12 and 13:

$$H_T^\circ - H_{298}^\circ = \int_{298}^{330} C_p dT + \Delta H_{melting}^\circ + \int_{330}^{588} C_p' dT + \Delta H_{evaporation}^\circ + \int_{558}^{T} C_p'' dT \quad \text{(Eq 12)}$$

$$S_T^\circ - S_{298}^\circ = \int_{298}^{330} \left(\frac{C_p}{T}\right) dT + \frac{\Delta H_{melting}^\circ}{330} + \int_{330}^{588} \left(\frac{C_p'}{T}\right) dT + \frac{\Delta H_{evaporation}^\circ}{588} + \int_{558}^{T} \left(\frac{C_p''}{T}\right) dT \quad \text{(Eq 13)}$$

The standard Gibbs energy change can be determined from the measured standard enthalpy and entropy changes using Eq 14[13]:

$$G_T^\circ - G_{298}^\circ = (H_T^\circ - H_{298}^\circ) - T(S_T^\circ - S_{298}^\circ) \quad \text{(Eq 14)}$$

The enthalpy of melting and evaporation can be calculated from the corresponding DTA peak area, since DTA peak area is proportional to enthalpy change of phase transition.[14] The area under DTA curve can be represented as $A = \int D dT$ and the enthalpy change (ΔH) can be determined using Eq 15:

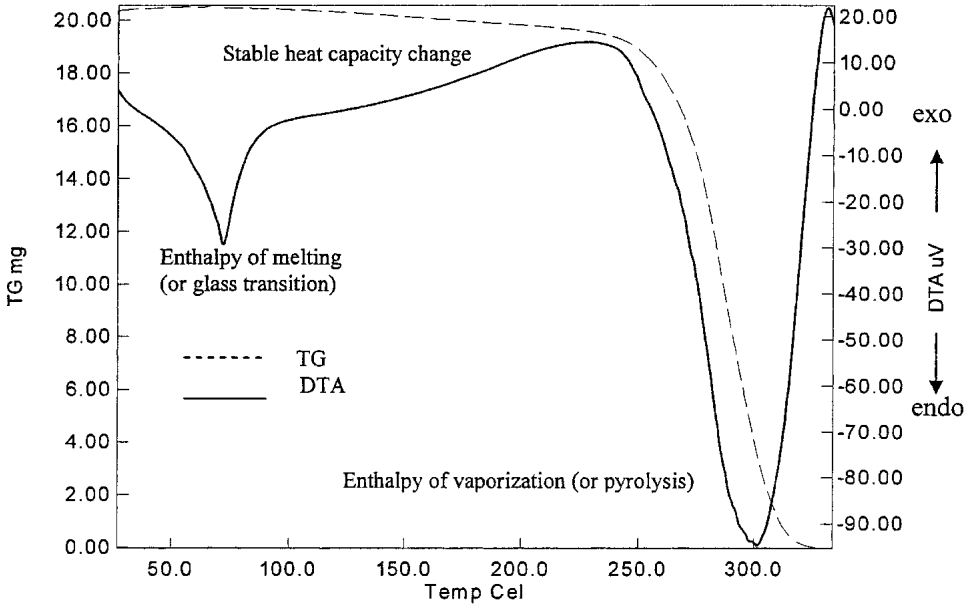

Fig. 3 TG and DTA curves for C_4mim[Cl] with dynamic argon purge at 100 cm^3/min and 10 °C/min temperature scan

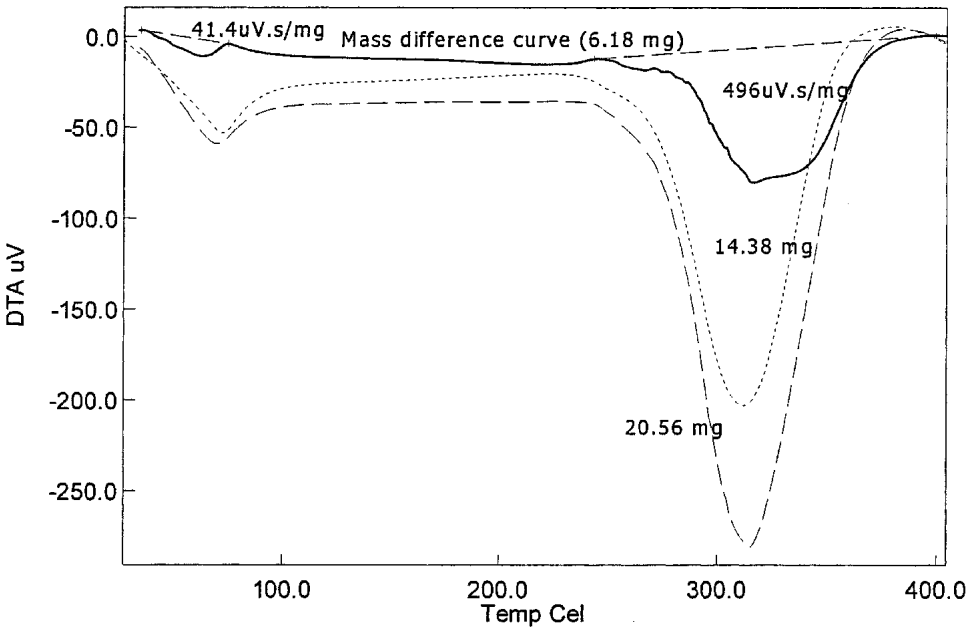

Fig. 4 Heat capacity measurements of C_4mim[Cl] using the mass difference baseline method

$$\Delta H^\circ = \int \mathrm{d}H = \int \frac{K_2}{K_2'} \frac{(\mathrm{d}H/\mathrm{d}T)'}{D'} D \cdot \mathrm{d}T = \frac{K_2}{K_2'} \frac{(\mathrm{d}H/\mathrm{d}T)'}{D'} A = \frac{K_2}{K_2'} \frac{(C_\mathrm{p})'}{D'} A \quad \text{(Eq 15)}$$

The enthalpy of phase changes such as melting ($\Delta H^\circ_{\mathrm{melting}}$) and evaporation ($\Delta H^\circ_{\mathrm{evaporation}}$) can be determined from Eq 15. The enthalpy of melting of C_4mim[Cl] ionic liquid is given by Eq 16:

$$\Delta H^\circ_{\mathrm{melting}} = \left(\frac{K_2}{K_2'}\right)_{380\mathrm{K}} \frac{C^\circ_{\mathrm{p,380K}}}{D_{380\mathrm{K}}} A_{\mathrm{melting}} \quad \text{(Eq 16)}$$

Here, $(K_2/K_2')_{380\mathrm{K}}$ is the conversion factor of α-sapphire at 380 K, $C^\circ_{\mathrm{p,380K}}$ is the heat capacity of C_4mim[Cl] determined previously, $D_{380\mathrm{K}}$ is the numerical value of the DTA signal, and A_{melting} is the area of the endothermic peak at the melting point of C_4mim[Cl]. From Fig. 4, the area of the DTA peak at the melting point was found to be 41.4 μv

s/mg, and the corresponding enthalpy of melting was determined as 0.93 kJ/mol. Similarly, the enthalpy of evaporation was calculated as 11.07 kJ/mol from the DTA peak area of 496 μv s/mg at the evaporation temperature.

Table 2 Heat capacity of C_4mim[Cl] calculated using DTA (this study) and DSC methods (literature)

T, K	C_p^o, (DTA), J/mol K	C_p^o (DSC)[3], J/mol K
298	275.98	275.98(a)
313	285.07	283.08(a)
323	291.14	288.15(a)
330	295.17	291.43(a)
340	306.57	296.66
343	307.95	297.14
353	312.55	303.55
360	315.73	307.42
370	320.37	312.15
380	329.86	317.90
393	330.95	323.79
400	336.17	326.63
413	340.15	333.91
420	340.37	337.11
423	344.75	338.19
433	349.35	344.03
440	352.57	347.59
453	358.55	354.15

(a) Extrapolated from higher temperature data.

4. Results and Discussion

The heat capacities of C_4mim[Cl], determined by the DTA mass difference baseline method in this study and that determined using DSC obtained from the literature[3] are listed in Table 2. The heat capacity data determined in the current study varied by about ±3% from the literature data.[3] The disparity in heat capacities may be attributed to different measuring techniques and the purity of ionic liquid. Generally, DSC measurement requires a constant sample mass and is encapsulated in a sample holder; however, in the case of DTA, the sample is uncovered and its mass changes with temperature.

The heat capacity of C_4mim[Cl] was found to increase linearly on either sides of the melting point. Thus, the heat capacity data was modeled to a linear expression of the form $\alpha + 2\beta T$; the regression constants α, β are shown in Table 3 for two temperature ranges. However, the changes in standard enthalpy, entropy and Gibbs energy of C_4mim[Cl] were derived from the heat capacity. The deduced expressions and regression constants for the standard thermodynamic quantities are listed in Table 3.

Kabo et al. have studied thermodynamic properties of 1-butyl-3-methylimidazolium hexafluorophosphate in condensed phases using adiabatic calorimetry.[15] Heat capacities for C_4mim[PF_6] were reported in the range of 5-550 K and were fitted to a polynomial equation of the form $C_p = a + bT + cT^2$ in contrast to a linear relationship $y = k + aT$ reported by Holbrey.[3] In the current study, the heat capaci-

Table 3 Thermodynamic properties of C_4mim[Cl] ionic liquid in the temperature range of 298–453 K

T, K	C_p^o, J/mol K	$H^o - H^o_{298}$, J/mol	$S^o - S^o_{298}$, J/mol K	$G^o - G^o_{298}$, J/mol
298	275.98	0.00	0.00	0.00
313	285.07	4202.25	13.76	−104.56
323	291.14	7078.75	22.81	−287.47
330	295.17	9128.00	29.08	−469.10
330	301.97	10,054.00	31.88	−466.32
340	306.57	13,096.70	40.96	−830.64
343	307.95	14,018.48	43.66	−957.58
353	312.55	17,120.98	52.58	−1438.88
360	315.73	19,320.10	58.75	−1828.55
370	320.37	22,500.80	67.46	−2459.68
380	329.86	25,727.50	76.07	−3177.40
393	330.95	29,990.98	87.10	−4238.14
400	336.17	32,318.90	92.97	−4868.39
413	340.15	36,701.98	103.75	−6147.23
420	340.37	39,094.30	109.50	−6893.62
423	344.75	40,126.48	111.94	−7225.78
433	349.35	43,596.98	120.05	−8385.83
440	352.57	46,053.70	125.68	−9245.92
453	358.55	50,675.98	136.03	−10,947.20
Fitted equation	$\alpha + 2\beta T$	$\lambda + \alpha T + \beta T^2$	$\theta + \alpha \ln T + 2\beta T$	$\lambda + (\alpha - \theta)T - \alpha T \ln T - \beta T^2$
ΔT	298 – 330 K 96.85 + 0.60*T*	−55,502.50 + 96.85*T* + 0.30T^2	−730.56 + 96.85 ln *T* + 0.60*T*	−55,502.50 + 827.41 *T* − 96.85*T* ln *T* − 0.30T^2
	330 – 453 K 150.17 + 0.46*T*	−64,549.10 + 150.17*T* + 0.23T^2	−990.77 + 150.17 ln *T* + 0.46 *T*	−64,549.10 + 1140.94*T* − 150.17*T* ln *T* − 0.23T^2

Phase change: 330 K, melting point of C_4mim[Cl]; $\Delta H^o_{melting} = 0.93$ kJ/mol

ties of C_4mim[Cl] exhibited linear relationship with temperature on either sides of melting point. However, the standard enthalpy, entropy, and Gibbs energy changes calculated from heat capacity varied nonlinearly with temperature.

5. Conclusions

The heat capacity and enthalpy change of phase transformation for C_4mim[Cl] ionic liquid were measured over the temperature range 298-453 K using the DTA mass difference baseline method. The heat capacity of C_4mim[Cl] measured in this study compared well with that reported in the literature. Thermodynamic properties such as standard enthalpy, entropy, and Gibbs energy change were then determined from the heat capacity data over the measured range of 298-453 K. The heat capacities of C_4mim[Cl] exhibited linear behavior on either sides of the melting point. However, the standard enthalpy, entropy and the standard Gibbs energy changes exhibited nonlinear behavior. The enthalpy of melting and the enthalpy of vaporization were determined as 0.93 and 11.07 kJ/mol, respectively.

Acknowledgments

The authors would like to acknowledge the financial support for the present research by National Renewable Energy Laboratory (NREL), National Science Foundation (NSF-ECS-0099853), United States Department of Energy (DE-FC07-02ID14397), and The University of Alabama. We would like to thank Mr. Ravinder N. Reddy for his guidance in synthesizing the ionic liquids.

References

1. T. Welton, Room Temperature Ionic Liquids for Synthesis and Catalysis, *Chem. Rev.,* Vol 99, 1999, p 2071-2083
2. J.G. Huddleston, A.E. Visser, W.M. Reichert, H.D. Willauer, G.A. Broker, and R.D. Rogers, Characterization and Comparison of Hydrophilic and Hydrophobic Room Temperature Ionic Liquids Incorporating the Imidazolium Cation, *Green Chemistry,* Vol 3, 2001, p 156-164
3. J.D. Holbrey, W.M. Reichert, R.G. Reddy, and R.D. Rogers, Heat Capacities of Ionic Liquids and Their Applications as Thermal Fluids, *Ionic Liquids as Green Solvents: Progress and Prospects,* R.D. Rogers and K.R. Seddon, Ed., ACS Symposium Series Vol 856, American Chemical Society, New York, 2003, p 121-133
4. R.G. Reddy, Z. Zhang, M.F. Arenas, and D.M. Blake, Thermal Stability and Corrosivity of Ionic Liquids as Thermal Energy Storage Media, *High Temp. Mater. Proc.,* Vol 22, 2003, p 87-94
5. Z. Zhang and R.G. Reddy, Thermal Stability of Ionic Liquids, *Fundamentals of Advanced Materials for Energy Conversion,* D. Chandra and R.G. Bautista, Ed., EPD Congress, The Minerals, Metals and Materials Society (TMS), Warrendale, PA, 2002, p 33-39
6. J. Yang and C. Roy, Using DTA to Quantitatively Determine Enthalpy Change Over a Wide Temperature Range by the Mass-Difference Baseline Method, *Thermochim. Acta,* Vol 333, 1999, p 131-140
7. J. Yang and C. Roy, A New Method for DTA Measurement of Enthalpy Change During the Pyrolysis of Rubbers, *Thermochim. Acta,* Vol 288, 1996, p 155-168
8. J.S. Wilkes, J.A. Levisky, R.A. Wilson, and C.L. Hussey, Dialkylimidazolium Chloroaluminate Melts: A New Class of Room-Temperature Ionic Liquids for Electrochemistry, Spectroscopy, and Synthesis, *Inorg. Chem.,* Vol 21, 1982, p 1263-1264
9. P. Wasserchеid and T. Welton, *Ionic Liquids in Synthesis,* Ed., Wiley-Vch Verlag, Weinheim, Germany, 2003, p 7-19
10. M.J. Vold, Differential Thermal Analysis, *Anal. Chem.,* Vol 21, 1949, p 683
11. W.J. Smothers and Y. Chiang, *Handbook of Differential Thermal Analysis,* Chemical Publishing Company, 1966, p 90-98
12. T. Hatakeyama and Z. Liu, *Handbook of Thermal Analysis,* 1st ed., John Wiley & Sons, UK, 1984, p 424
13. N.A. Gokcen and R.G. Reddy, *Thermodynamics,* 2nd ed., Plenum Press, New York, 1996
14. T. Hatakeyama and Z. Liu, *Handbook of Thermal Analysis,* 1st ed., John Wiley & Sons, UK, 1998 p 9-10
15. G.J. Kabo, A.V. Blokhin, Y.U. Paulechka, A.G. Kabo, and M.P. Shymanovich, Thermodynamic properties of 1-butyl-3-methylimidazolium Hexafluorophosphate in Condensed State, *J. Chem. Eng. Data,* Vol 49, 2004, p 453-461